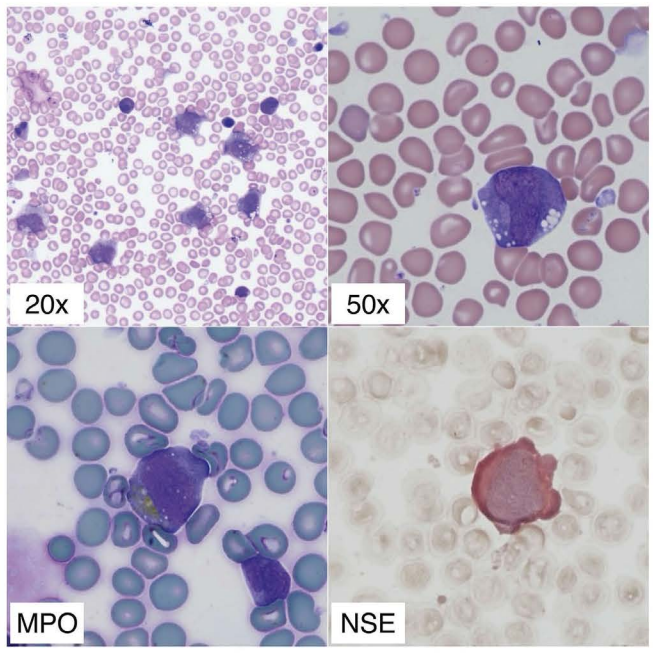
# Novel *KAT6B::NUTM2B* fusion oncogene in congenital acute myeloid leukemia and implications for menin inhibitor therapy

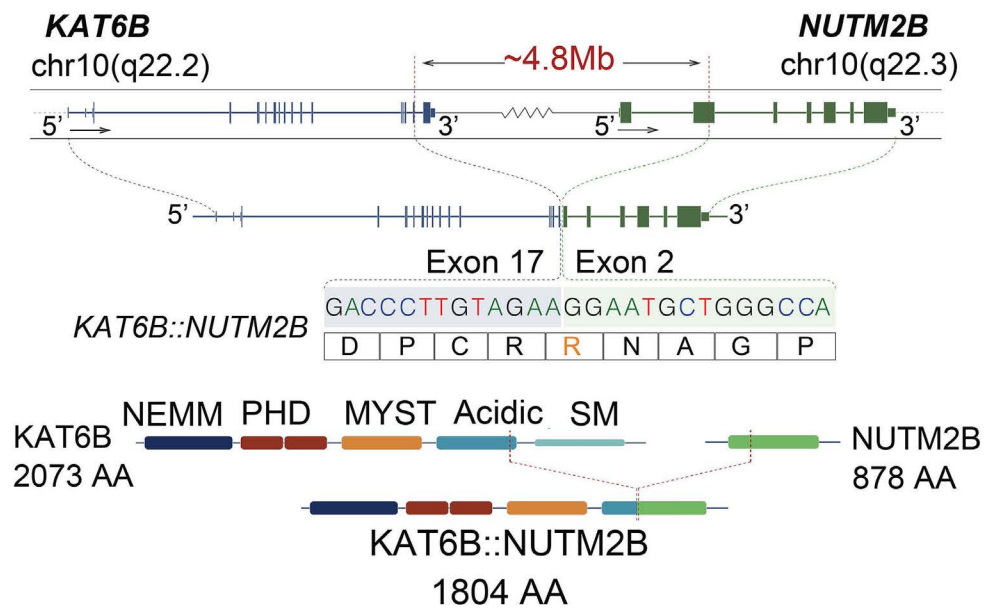
Congenital acute myeloid leukemia (AML) is rare and may initially present as myeloid sarcoma. The most common non-Down syndrome-related congenital leukemia is AML, with over half involving *KMT2A* or *KAT6A* fusions.[1,2] *KMT2A*-rearranged infant AML has a poor prognosis, while some cases with *KAT6A* fusions may spontaneously remit.[2] Studies of molecular pathogenesis have revealed a functional connection between *KMT2A* and *KAT6A* in transcriptional activation. Both KMT2A and KAT6A fusion proteins drive aberrant transcription and self-renewal in hematopoietic progenitors, notably activating *HOXA* genes.[3,4] Inhibitors targeting the KMT2A/KAT6A transcriptional complex, especially menin inhibitors, have shown therapeutic promise.[5,6] Here, we report the identification of a novel *KAT6B::NUTM2B* fusion, involving the *KAT6A* paralog *KAT6B*, in congenital AML and demonstrate its oncogenic activity and sensitivity to menin inhibition through *in vitro* studies in mouse hematopoietic stem and progenitor cells (mHSPC). Informed consent for clinical genomics testing was obtained from the patient's legal guardians, and this study was approved by the Institutional Review Board at St. Jude Children's Research Hospital (SJCRH). The findings expand the knowledge of *KAT6A/B*-rearranged AML and suggest menin inhibitors as a potential therapy.

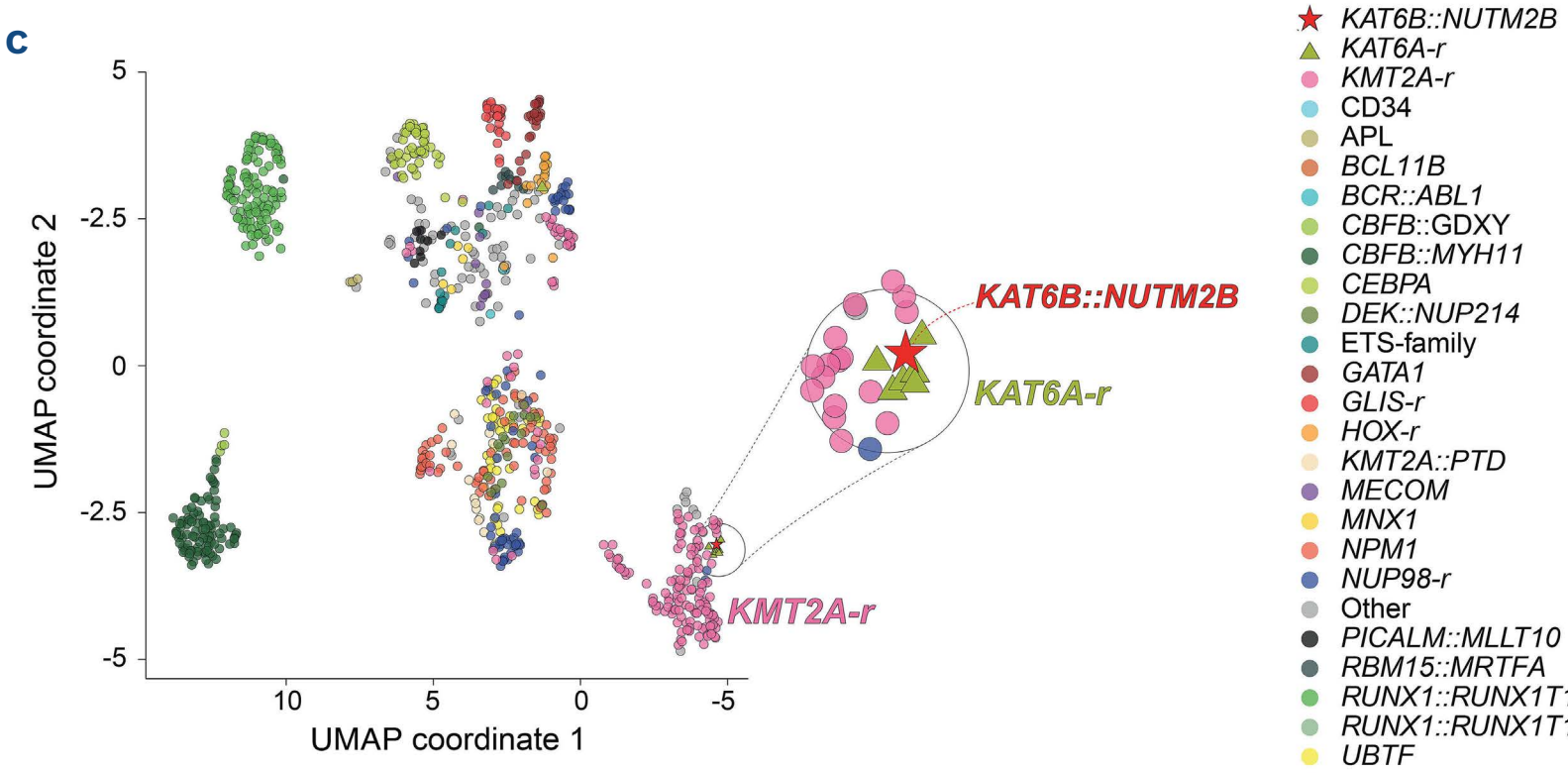
The patient presented with a blueberry muffin rash at birth. A biopsy of the rash revealed myeloid sarcoma. A bone marrow sample collected at day 9 after birth showed 37% blasts, positive for MPO and NSE (Figure 1A), and flow cytometry indicated AML with monocytic differentiation (positive for CD11c, CD64, CD33, HLA-DR, CD123, and MPO; CD14 loss in most blasts; negative for CD34, CD117, CD133, NG2, CD19, and CD3) (*Online Supplementary Figure S1A*). No clonal abnormalities or *KMT2A* rearrangement were detected by karyotyping or fluorescence *in situ* hybridization. Bone marrow aspirate and biopsy samples of skin lesions were collected for molecular diagnosis in a CLIA-certified laboratory at SJCRH. The fresh bone marrow aspirate was subjected to DNA and RNA extraction followed by clinical genomics testing as previously described,[7] including whole-genome sequencing and whole-transcriptome sequencing. Formalin-fixed paraffin-embedded tissue of a skin lesion biopsy was subjected to RNA extraction and whole-transcriptome sequencing only. Integrated whole-genome sequencing and whole-transcriptome sequencing analyses identified a cryptic deletion at chromosome region 10q22 resulting in an in-frame *KAT6B::NUTM2B* fusion, preserving the exons encoding the histone acetyltransferase domain of *KAT6B* and most of the coding sequence of *NUTM2B* (Figure 1B). This fusion was the only tumor-acquired likely pathogenic alteration identified and was also detected in the skin rash by whole-transcriptome sequencing. Transcriptomic profiling clustered the case with *KAT6A*- and *KMT2A*-rearranged AML (Figure 1C) and high expression of *HOXA9* and *HOXA10* was observed (Figure 1D). An initial watch-and-wait management was chosen due to possible spontaneous remission.[1] At 4 months of age, disease progressed (44% blasts in bone marrow, hemophagocytosis), prompting standard pediatric induction chemotherapy (*Online Supplementary Figure S1B*) and subsequent haploidentical stem cell transplant. Full donor engraftment was achieved and the bone marrow was negative for measurable residual disease by flow cytometry, a status sustained for several months after the transplant. Relapse occurred at 1 year (77.6% blasts, testicular myeloid sarcoma). Unfortunately, the patient died at 16 months despite further chemotherapy.

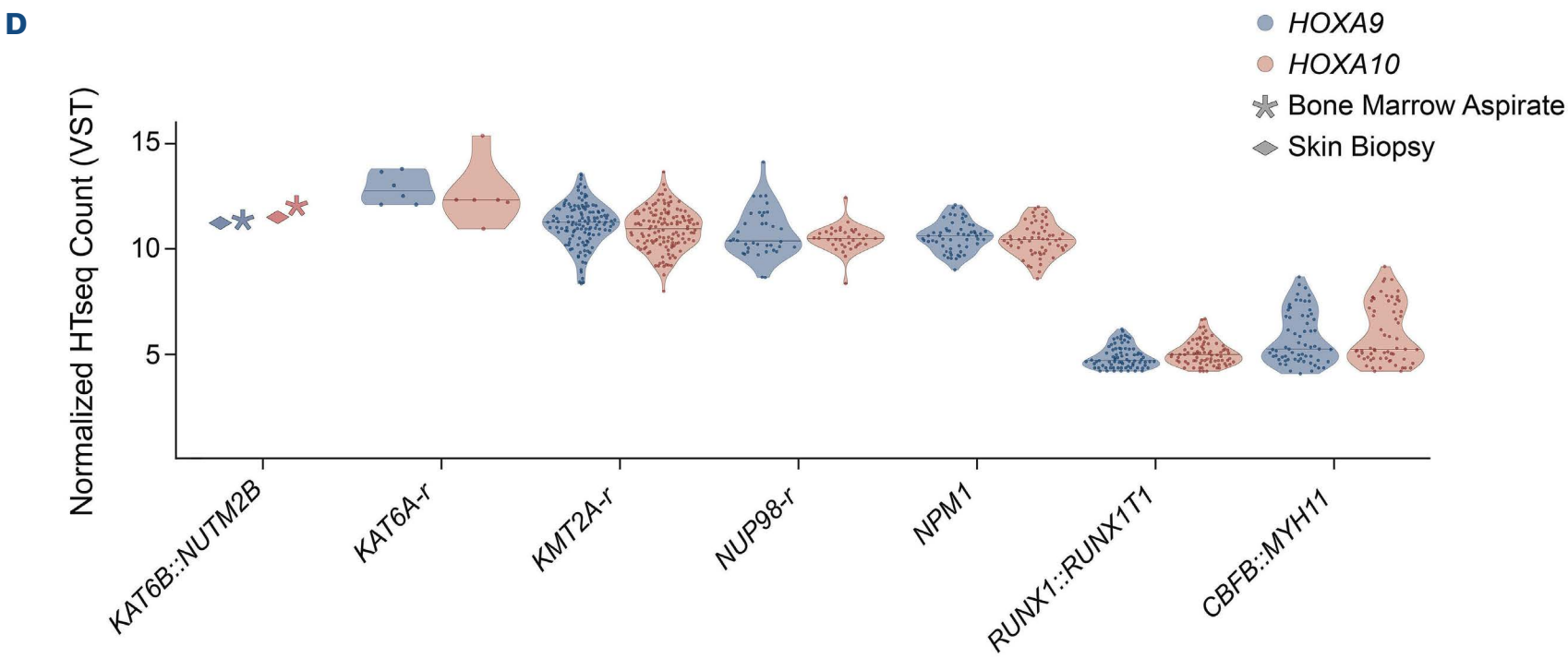
To our knowledge, this patient represents the first reported case in an infant and the fifth case of a myeloid malignancy harboring a *KAT6B* gene fusion, as well as the first reported instance of a *KAT6B::NUTM2B* fusion. The four previously reported cases all carried a *KAT6B::CREBBP* fusion, which is considered a variant of *KAT6A::CREBBP* (*Online Supplementary Table S1*). *KAT6A::CREBBP* is a rare but recurrent AML-defining fusion,[8] with other *KAT6A* fusion partners (*NCOA2*, *NCOA3*, *EP300*, *LEUTX*, *ASXL2*) also reported in myeloid malignancies (*Online Supplementary Table S1*). Review of infant AML with *KAT6A* fusions shows that over 80% of patients presented with skin lesions (myeloid sarcoma). Bone marrow involvement typically showed morphological features consistent with AML French-American-British subtype M4 or M5, with erythrophagocytosis observed in up to 50% of cases. Hepatosplenomegaly was frequently present, and up to 30% of patients showed disseminated intravascular coagulation. Spontaneous remission occurred in up to 45% of congenital AML patients with *KAT6A* rearrangements. Overall, the current case with a novel *KAT6B::NUTM2B* fusion shares clinical features similar to those observed in infant AML with *KAT6A* fusions; however, despite remaining clinically stable with improvement of skin lesions for approximately 4 months without treatment, the patient ultimately had a poor clinical outcome.

To gain deeper insights into the novel *KAT6B::NUTM2B* fusion, the full-length coding sequence of the *KAT6B::NUTM2B* fusion as well as controls (wild-type *KAT6B* and *NUTM2B*) were cloned into MSCV-IRES-GFP (MPG) lentiviral expression



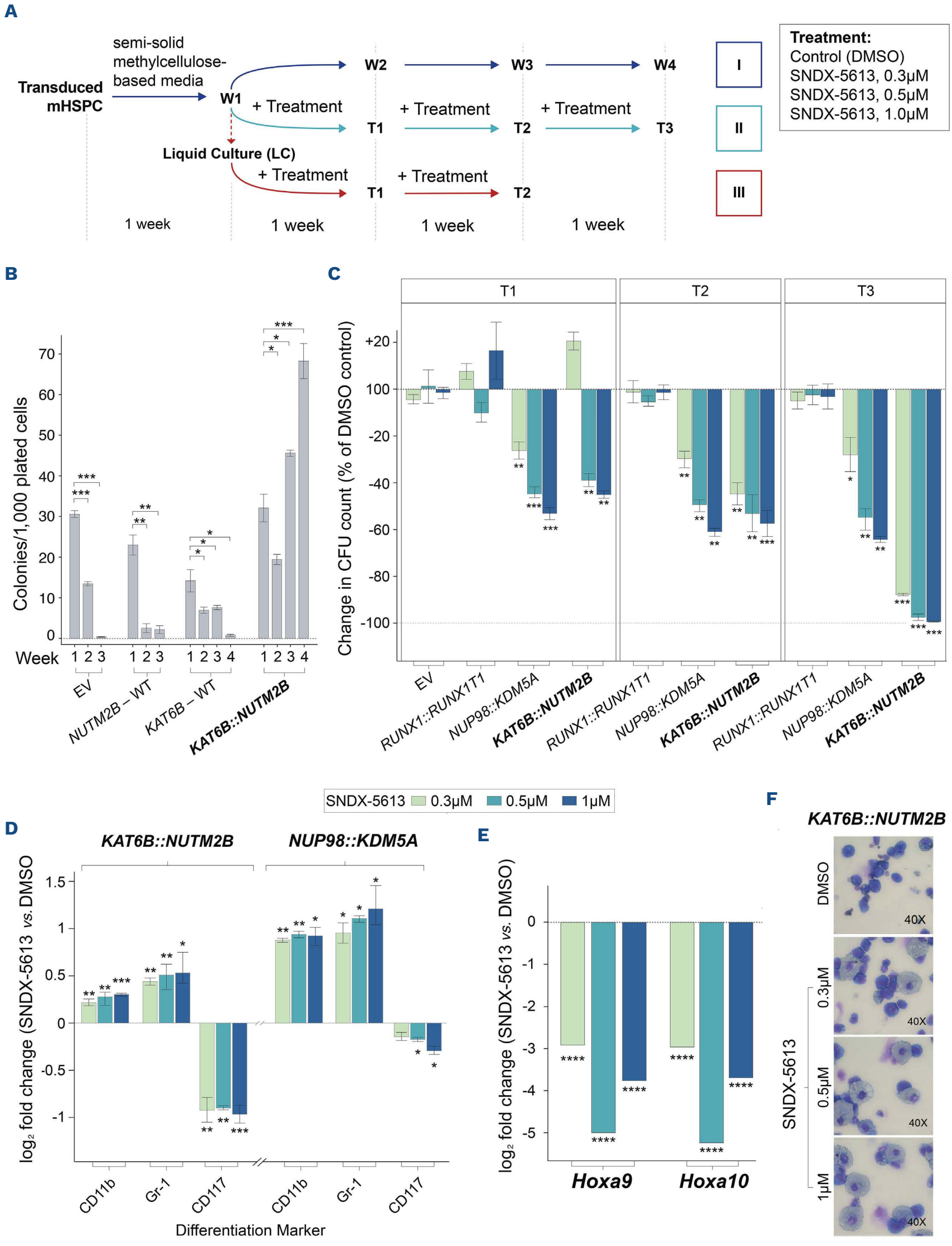




Continued on following page.

**Figure 1. Diagnostic workup of the patient's bone marrow sample.** (A) Morphology and immunohistochemical staining of diagnostic bone marrow. Upper panels: Wright-Giemsa staining captured at 20x and 50x magnification highlights blasts. Lower panels: immunohistochemical staining for myeloperoxidase and neuron-specific enolase shows reactivity in blasts. (B) Identification of the novel *KAT6B::NUTM2B* fusion in the diagnostic bone marrow sample. Upper part: schema of *KAT6B* (NM_012330) and *NUTM2B* (NM_001278495) gene structures as well as the cryptic deletion of approximately 4.8 Mb in relation to the formation of the *KAT6B::NUTM2B* fusion, followed by a partial sequence of the *KAT6B::NUTM2B* fusion transcript along with the predicted amino acid sequence. The transcript is an in-frame fusion of *KAT6B* exon 17 to *NUTM2B* exon 2 (mid-exon). Lower part: schematic diagrams of KAT6B, NUTM2B and the predicted KAT6B::NUTM2B chimeric proteins with their functional domains: N-terminal extension of MYST; plant homeodomain; histone acetyltransferase domain; acidic domain (transcriptional activation and interaction with co-activators) and a serine-methionine-rich region. (C) Global gene expression profiling. Global gene expression profiling was conducted using uniform manifold approximation and projection (UMAP) analysis as previously described (doi:10.1038/s41588-023-01640-3). The *KAT6B::NUTM2B*-positive case clustered with the *KAT6A*-rearranged and *KMT2A*-rearranged subtypes by UMAP. The UMAP plot was generated in the context of a previously published cohort of pediatric acute myeloid leukemia (AML) (N=887, doi:10.1038/s41588-023-01640-3) and cord blood $CD34^+$ cells (N=5). (D) Normalized expression of *HOXA9* and *HOXA10* genes. Expression levels are shown for the *KAT6B::NUTM2B*-positive patient along with reference cases from selected AML subtypes, including molecular categories known to be associated with *HOXA* activation (*KAT6A*-rearranged, *KMT2A*-rearranged, *NUP98*-rearranged and *NPM1*-mutated) and those that do not have *HOXA* activation (*RUNX1::RUNX1T1* and *CBFB::MYH11*). The reference cases (N=374) were available from St. Jude Cloud (*https://www.stjude.cloud*) and were included in a previously published pediatric AML study cohort (doi:10.1038/s41588-023-01640-3). Expression values are shown as variance-stabilized counts derived from HTSeq counts as previously described.[7] AA: amino acids; MPO: myeloperoxidase; MYST: histone acetyltransferase domain; NEMM: N-terminal extension of MYST; NSE: neuron-specific enolase; PHD: plant homeodomain; SM: serine-methionine-rich region; VST: variance-stabilized counts.

vector and transduced into C57BL/6J murine bone marrow mHSPC to assess the transforming properties of *KAT6B::NUTM2B*. Initially, *Hoxa9* and *Hoxa10* mRNA were assessed in mHSPC expressing either wild-type *KAT6B* (*KAT6B*-mHSPC) or *KAT6B::NUTM2B* (*KN*-mHSPC). Consistent with elevated *HOXA9/10* expression observed in the patient's leukemia sample, there was a significant upregulation of *Hoxa9* and *Hoxa10* in *KN*-mHSPC (*Online Supplementary Figure S2B*). The mHSPC transduced with *KAT6B::NUTM2B* or controls were plated in semi-solid methylcellulose-based media for colony-forming unit assay. Colonies were counted, harvested, and serially replated every 7 days (Figure 2A-I). The *KN*-mHSPC exhibited a significant and sustained increase in colony formation, with successful serial replating for 4 weeks or longer, in contrast to wild-type *KAT6B* or *NUTM2B*, or empty vector controls (Figure 2B). Considering the *HOXA9/10* activation in the patient's leukemia, *KN*-mHSPC were treated with SNDX-5613, a clinical-grade menin inhibitor, at three different concentrations over a 3-week period (Figure 2A-II and III). We evaluated the sensitivity of the *KAT6B::NUTM2B* fusion to SNDX-5613 in comparison with two common fusions in pediatric AML: *RUNX1::RUNX1T1* (9a isoform[9]) serving as a negative control as it is not considered a primary target of menin inhibitors, and *NUP98::KDM5A*, which is associated with *HOXA* activation and sensitivity to menin inhibitors,[10] serving as a positive control. An empty vector control was also included. By the end of week 3, colony formation of *KN*-mHSPC was reduced by approximately 90-95% with SNDX-5613 treatment at all three concentrations, *NUP98::KDM5A*-transduced cells also exhibited a dose-dependent reduction in colony formation with SNDX-5613, albeit less prominently than *KN*-mHSPC. In contrast, no significant change was seen in controls (empty vector or *RUNX1::RUNX1T1*-transduced cells) (Figure 2C). Besides the reduction of clonogenic growth, SNDX-5613 treatment resulted in a significant increase in Gr1 and CD11b positivity and a concomitant decrease in CD117 (cKIT) expression in both *KAT6B::NUTM2B* and *NUP98::KDM5A* transduced mHSPC, indicating myeloid maturation and loss of stemness (Figure 2D). Additionally, menin inhibition resulted in significantly reduced *Hoxa9/10* mRNA expression (Figure 2E) and morphological changes in *KN*-mHSPC (Figure 2F).

Both *KAT6A* and *KAT6B* encode histone acetyltransferases (HAT) that are core components of the MOZ/MORF complex[11] and closely interact with the KMT2A (a.k.a. MLL) complex, facilitating histone acetylation and cooperatively promoting transcription of genes regulating hematopoiesis.[3] While wild-type *KAT6A* and *KAT6A* fusions have been functionally characterized, the role of *KAT6B* in hematopoiesis has only recently been recognized.[12] Fusions involving *KAT6A* or *KAT6B* retain 5' exons encoding the MYST (histone acetyltransferase) domain (Figure 3), thereby preserving N-terminal functional domains of KAT6A/B in the resulting chimeric proteins. Notably, nearly all previously reported fusion partners of *KAT6A/B* are transcriptional co-activators (such as *CREBBP*, *EP300*, *NCOA2*, *NCOA3*) or are predicted to possess a transcriptional activation domain (e.g., *LEUTX*), with these activation domains consistently retained as C-terminal regions in the fusion proteins. Consequently, *KAT6A/B* fusions typically contain one or more HAT domains capable of modifying chromatin and activating genes such as the *HOXA* cluster. While *NUTM2B* has been reported in *YWHAE::NUTM2B* fusion in sarcomas, the function of wild-type *NUTM2B* is unclear. Interestingly, a recent study reported that YWHAE::NUTM2B can interact with EP300 and CREBBP.[13] Although the specific functional domain mediating the interaction with EP300/CREBBP was not elucidated in the study of YWHAE::NUTM2B, it raises the possibility that KAT6B::NUTM2B may similarly recruit these co-activators to promote the transcription of *HOXA* genes, akin to *KAT6A/B::NCOA2* fusions.




Continued on following page.

**Figure 2. *In vitro* studies with *KAT6B::NUTM2B*-transduced murine bone marrow hematopoietic stem and progenitor cells.** (A) Schematic depiction of workflow. GFP⁺-transduced cells were sorted and plated in methylcellulose for 1 week (W1). After this initial incubation, cells were divided as follows: (i) to continue colony-forming unit (CFU) assays without (I) and with (II) SNDX-5613 treatment, and (ii) to assess the effects of SNDX-5613 treatment in liquid culture (III). (B) CFU assay. Transduced murine bone marrow hematopoietic stem and progenitor cells (mHSPC) were plated in triplicate in methylcellulose ($2\times10^4$ cells/35 mm dish). Colonies were counted and serially replated every 7 days. Results from one representative CFU assay are presented, with similar findings observed across multiple independent repeats. (C) Impact of SNDX-5613 treatment on colony formation in the CFU assay. Results are shown from a representative experiment (1 of 4 independent replicates) conducted as outlined in Figure 2A-II. Transduced mHSPC were plated in methylcellulose and treated with SNDX-5613 at 0.3 μM, 0.5 μM, or 1.0 μM, or with 0.1% dimethylsulfoxide (DMSO) as a control. Treatment with the indicated concentrations of SNDX-5613 started after the initial 1-week incubation in semi-solid culture. The process continued for 3 weeks, with cells replated and treated in fresh methylcellulose every 7 days. Colonies were counted prior to each replating. The x-axis shows time points after 1, 2, and 3 weeks of treatment (T1, T2, T3). The y-axis shows the relative change in CFU counts compared to the DMSO control (% of DMSO control). Error bars represent the standard deviation. Statistical significance was assessed using a two-sided Welch *t* test. **P*<0.05; ***P*<0.01; ****P*<0.001. (D) Flow cytometry analysis of myeloid differentiation markers. The mHSPC transduced with *KAT6B::NUTM2B* and *NUP98::KDM5A* were treated with SNDX-5613 at three concentrations or DMSO (control) in liquid culture (RPMI with cytokines) as outlined in Figure 2A-III. Results from a representative experiment are depicted. Bar plots display the $\log_2$ fold change in mean fluorescence intensity for CD11b, Gr-1 and CD117, compared to their expression in transduced mHSPC treated with DMSO control (SNDX-5613 *vs*. DMSO). Statistical significance was assessed using a one-sided Welch *t* test based on the expected direction of change for each marker, **P*<0.05; ***P*<0.01; ****P*<0.001. (E) SNDX-5613 treatment reduced *Hoxa9* and *Hoxa10* expression at the transcriptional level. The mRNA expression of *Hoxa9* and *Hoxa10* in *KAT6B::NUTM2B*-transduced mHSPC was significantly downregulated by SNDX-5613 treatment compared with DMSO treatment (control). Cells in liquid culture were harvested after 1 and 2 weeks of treatment (T1 and T2, see Figure 2A-III); results are shown for T2. Bars represent $\log_2$ fold change (SNDX-5613 treated *vs*. DMSO) for *Hoxa9* and *Hoxa10*. Statistical significance was assessed using a one-sided Welch *t* test (expected decrease). *****P*<0.0001. (F) Wright-Giemsa stained cytospins of *KAT6B::NUTM2B*-transduced cells obtained from the CFU assay harvested after 1 week of SNDX-5613 treatment (T1) as illustrated in Figure 2A-II. Images are shown at 40X magnification. EV: empty vector; WT: wild-type.

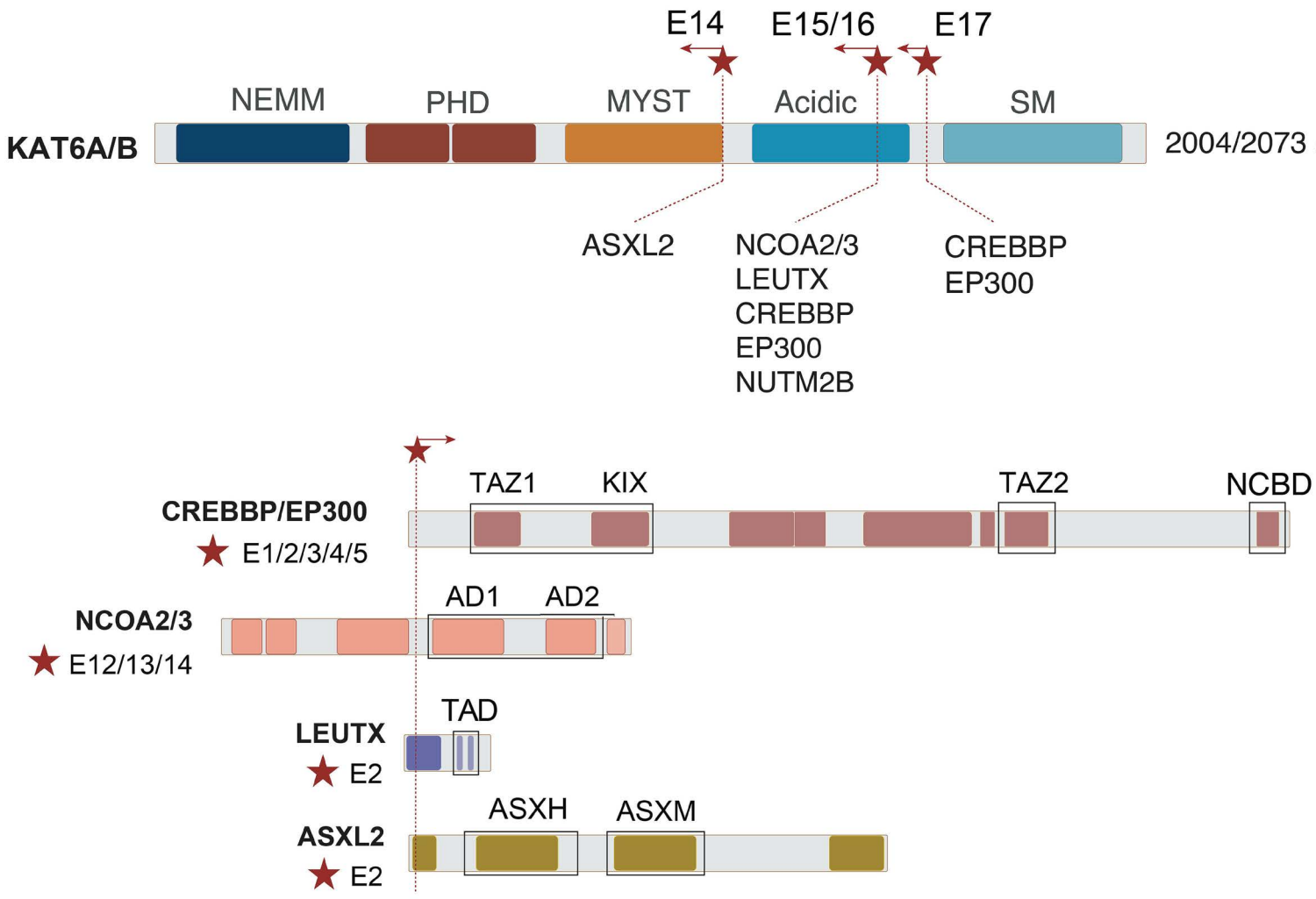



**Figure 3. Schematic representation of KAT6A or KAT6B fusion proteins.** Upper part: KAT6A/B with known fusion junctions associated with different fusion partners. In all chimeric proteins, the N-terminal region of KAT6A/B is retained, including the MYST domain which mediates histone acetyltransferase activity. Lower part: C-terminal fusion partners to KAT6A and/or KAT6B reported in literature. Fusion junctions are indicated by red stars. Black boxes highlight retained transcriptional activation domains in all fusion partners. aa: amino acids; AD: activation domain; ASXH: Asx homology domain: E: exon; KIX: CREB/kinase inducible domain interacting domain; MYST: histone acetyltransferase domain; NCBD: nuclear coactivator binding domain; NEMM: N-terminal extension of MYST; PHD: plant homeodomain; SM: serine-methionine-rich region; TAD: transactivation domain; TAZ1/2: transcriptional adaptor zinc-binding domain 1/2.

Previous studies have shown that the KAT6A::NCOA2 fusion protein targets chromatin in a wild-type KMT2A-dependent manner.[3] Menin plays a central role by tethering the KMT2A complex to DNA[6] and recruiting KAT6A/B-fusion proteins.[3] Menin inhibitors have demonstrated therapeutic efficacy in *KMT2A*-rearranged AML,[14] and emerging evidence from other *HOXA*-activating AML, including *KAT6A*-rearranged[3] and *NUP98*-rearranged AML,[10] suggests a similar vulnerability. Consistent with this model, treating *KN*-mHSPC with the menin inhibitor SNDX-5613 impaired colony formation, promoted myeloid differentiation, and reduced *Hoxa9/10* expression, supporting menin dependency in *KAT6B::NUTM2B* leukemogenesis. Our findings align with a previous study on *KAT6A::NCOA2*[3] and further indicate that menin inhibition may hold therapeutic potential against *KAT6A/B*-rearranged AML. In this study, we report a novel *KAT6B::NUTM2B* fusion in a patient with congenital AML whose clinical and transcriptomic features resembled those of patients with *KAT6A::CREBBP*-positive infant AML, indicating a shared mechanism. The *KAT6B::NUTM2B* fusion drove oncogenic transformation *in vitro*, and *KN*-mHSPC were vulnerable to a menin inhibitor, supporting the therapeutic potential of menin inhibition in *KAT6B*-rearranged AML. Further studies utilizing primary leukemia samples from AML patients harboring *KAT6A/B*-fusions are required to validate these findings. Given the increasing recognition of resistance to menin inhibitors,[15] alternative therapeutic strategies, such as KAT6 inhibitors or combination therapies, should be investigated. Overall, our findings provide critical new insights into the biology of *KAT6B* fusions and indicate a therapeutic strategy for this rare leukemia.

## Authors

Rebecca K. Voss,[1] Wenqing Qi,[1] La'Ron Browne,[2] Ruth W. Wang'ondu,[2] Mahsa Khanlari,[1] Jing Ma,[1] Xuefei Ma,[1,3] Josi Lott,[4] Juan M. Barajas,[1] Melvin Thomas III,[1] Victor B. Pastor Loyola,[1] Hui Cao,[1] Larissa V. Furtado,[1] Swati Naik,[5] Sakshi Bami,[6] Seth E. Karol,[2] Jeffrey E. Rubnitz,[2] Jeffery M. Klco,[1] Yen-Chun Liu[1] and Lu Wang[1]

[1]Department of Pathology, St. Jude Children's Research Hospital, Memphis, TN, USA; [2]Department of Oncology, St. Jude Children's Research Hospital, Memphis, TN, USA; [3]Department of Laboratory Medicine, Ruijin Hospital, Shanghai Jiao Tong University School of Medicine, Shanghai, China; [4]Center of Excellence in Leukemia Studies, St. Jude Children's Research Hospital, Memphis, TN, USA; [5]Department of Bone Marrow Transplant and Cellular Therapy, St. Jude Children's Research Hospital, Memphis, TN, USA and [6]Department of Hematology/Oncology, St Jude Affiliate Clinic, Our Lady of the Lake Children's Hospital, Baton Rouge, LA, USA

Correspondence:
L. WANG - Lu.Wang2@stjude.org
Y-C. LIU - Yen-Chun.Liu@stjude.org

https://doi.org/10.3324/haematol.2025.300350

Received: December 10, 2025.
Accepted: April 10, 2026.
Early view: April 23, 2026.

©2026 Ferrata Storti Foundation
Published under a CC BY-NC license

**Disclosures**

No conflicts of interest to disclose.

**Contributions**

LW, Y-CL, and JMK designed the study. LW and Y-CL supervised the conduction of the project. L'RB, JER, RWW, MK, SN, SB, Y-CL, LW, LVF, and SEK contributed to the patient's care. Y-CL provided morphology and flow cytometry analyses of the patient's samples. VBPL analyzed the patient's whole-genome sequencing and whole-transcriptome data. JM conducted transcriptomic profiling of the patient's samples. RKV, WQ, XM, and JL conducted *in vitro* studies. JMB, MTIII, and HC provided material and expertise for conducting the *in vitro* studies. RKV generated tables and figures for the manuscript. RKV and LW wrote the manuscript. All authors reviewed and edited the manuscript.

**Acknowledgments**

We thank Paula Perez-Sanchez at SJCRH Center of Excellence for Leukemia Studies Flow Cytometry Core; and Maria Cardenas in the Department of Computation Biology for providing HOXA9/10 expression data of leukemia samples from St. Jude Cloud. We sincerely thank Dr. Yiping Fan from the Center for Applied Bioinformatics at SJRCH for his invaluable assistance with analysis of the RNA-sequencing data. We thank the staff of SJCRH Flow Cytometry and Cell Sorting Shared Resource (FCCSSR).

**Funding**

This work was funded by the ALSAC of SJCRH. The SJCRH Flow Cytometry and Cell Sorting Shared Resource (FCCSSR) is supported in part by ALSAC and National Cancer Institute grant P30 CA021765.

**Data-sharing statement**

Data are available on request from the corresponding authors.

## References

1. Calvo C, Fenneteau O, Leverger G, Petit A, Baruchel A, Mechinaud F. Infant acute myeloid leukemia: a unique clinical and biological entity. Cancers (Basel). 2021;13(4):777.
2. Coenen EA, Zwaan CM, Reinhardt D, et al. Pediatric acute

myeloid leukemia with t(8;16)(p11;p13), a distinct clinical and biological entity: a collaborative study by the International Berlin-Frankfurt-Munster AML study group. Blood. 2013;122(15):2704-2713.
3. Miyamoto R, Okuda H, Kanai A, et al. Activation of CpG-rich promoters mediated by MLL drives MOZ-rearranged leukemia. Cell Rep. 2020;32(13):108200.
4. Paggetti J, Largeot A, Aucagne R, et al. Crosstalk between leukemia-associated proteins MOZ and MLL regulates HOX gene expression in human cord blood CD34+ cells. Oncogene. 2010;29(36):5019-5031.
5. White J, Derheimer FA, Jensen-Pergakes K, et al. Histone lysine acetyltransferase inhibitors: an emerging class of drugs for cancer therapy. Trends Pharmacol Sci. 2024;45(3):243-254.
6. Schurer A, Glushakow-Smith SG, Gritsman K. Targeting chromatin modifying complexes in acute myeloid leukemia. Stem Cells Transl Med. 2025;14(2):szae089.
7. Voss RK, Pastor Loyola VB, Cardenas MF, et al. Clinical experience of using integrated whole genome and transcriptome sequencing as a framework for pediatric and adolescent acute myeloid leukemia diagnosis and risk assessment. Leukemia. 2025;39(12):2946-2956.
8. Li W. The 5th Edition of the World Health Organization Classification of Hematolymphoid Tumors. In: Li W, ed. Leukemia [Internet]. Brisbane (AU): Exon Publications, 2022. Chapter 1.
9. Thomas MIII, Qi WQ, Walsh MP, et al. Functional characterization of cooperating mutations in acute myeloid leukemia. Leukemia. 2024;38(5):991-1002.
10. Michmerhuizen NL, Heikamp EB, Iacobucci I, et al. KAT6A and KAT7 histone acetyltransferase complexes are molecular dependencies and therapeutic targets in NUP98-rearranged acute myeloid leukemia. Cancer Discov. 2025;15(10):2096-2116.
11. Ullah M, Pelletier N, Xiao L, et al. Molecular architecture of quartet MOZ/MORF histone acetyltransferase complexes. Mol Cell Biol. 2008;28(22):6828-6843.
12. Bergamasco MI, Ranathunga N, Abeysekera W, et al. The histone acetyltransferase KAT6B is required for hematopoietic stem cell development and function. Stem Cell Reports. 2024;19(4):469-485.
13. Brahmi M, Duc A, Vanacker H, et al. P435) oncogenic fusion YWHAE::NUTM2 disrupt EP300/BCOR interaction. https://ctos2023.eventscribe.net/fsPopup.asp?PosterID=604159&mode=posterInfo Accessed Apr 8, 2026.
14. Issa GC, Aldoss I, Thirman MJ, et al. Menin inhibition with revumenib for KMT2A-rearranged relapsed or refractory acute leukemia (AUGMENT-101). J Clin Oncol. 2025;43(1):75-84.
15. Gordon SJV, Perner F, MacPherson L, et al. Catalytic inhibition of KAT6/KAT7 enhances the efficacy and overcomes primary and acquired resistance to menin inhibitors in MLL leukemia. Cancer Discov. 2025;15(10):2117-2138.